TRANSITION RADIATION AND THE ČERENKOV EFFECT*

BY

E. OTT** AND J. SHMOYS

Polytechnic Institute of Brooklyn

A. Introduction. When a charge crosses the boundary between two regions with different electrical properties a burst of electromagnetic energy is radiated. This phenomenon is called transition radiation.

In a previous paper [1] the authors considered the problem of transition radiation of a line charge. The problem considered is illustrated in Fig. 1. As

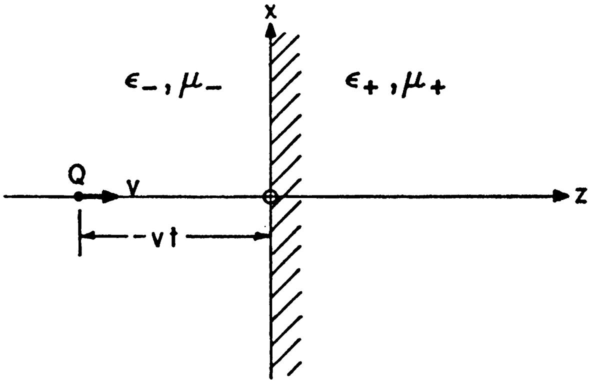

FIG. 1. Configuration for $t < 0$.

shown in Fig. 1, the line charge (of charge Q per unit length) moves with a constant velocity v and crosses a boundary between two dielectrics at the time $t = 0$. The dielectric constant is ϵ_+ for $z > 0$ and ϵ_- for $z < 0$. The magnetic permittivity is μ_+ for $z > 0$ and μ_- for $z < 0$.

In [1], v was assumed to be less than the speed of light in both media, i.e.

$$v < c_+ ,$$

and

$$v < c_- ,$$

where

$$c_\pm = (\mu_\pm \epsilon_\pm)^{-1/2}.$$

*Received April 17, 1967. Taken from the dissertation of Edward Ott submitted to the Faculty of the Polytechnic Institute of Brooklyn in partial fulfillment of the requirements for the degree of Doctor of Philosophy (Electrophysics), 1967. This research has been conducted under Contract No. NONR 839(38) and was made possible by the support of the Advanced Research Projects Agency under Order No. 529 through the Office of Naval Research.

**Present address: Cambridge University, Dept. of Applied Mathematics and Theoretical Physics, Cambridge, England.

Under these conditions no Čerenkov radiation is produced. In this paper we wish to consider the interesting problem of what happens when v is greater than the speed of light in either one or both of the media.

B. General Considerations. In general there are six cases:

case	c_+/c_-	v/c_+	v/c_-
1	<1	<1	<1
2	>1	<1	<1
3	<1	>1	<1
4	>1	<1	>1
5	<1	>1	>1
6	>1	>1	>1

Table I.

Cases 1 and 2 have already been dealt with in [1].

In case 3 the charge goes from a medium in which it produces no Čerenkov radiation to a medium in which it does. The solution for this case demonstrates how the Čerenkov radiation establishes itself after the impact time at $t = 0$.

In case 4 a charge producing Čerenkov radiation crosses into a region in which it produces no Čerenkov radiation. The situation for $t < 0$ is shown in Fig. 2.

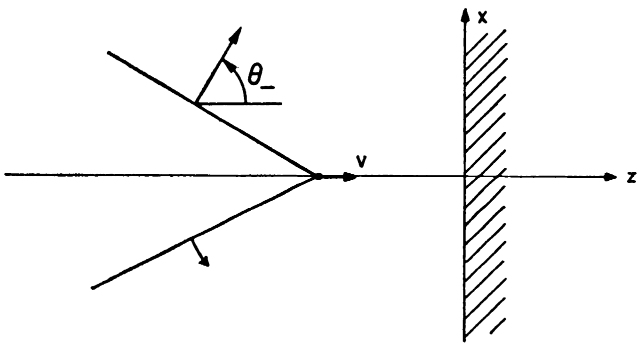

Fig. 2. Čerenkov radiation for $t < 0$.

The angle of the Čerenkov wedge is

$$\theta_- = \arccos (c_-/v). \tag{1}$$

After impact one expects the wavefronts to act like infinite plane waves incident on the boundary $z = 0$. For θ_- less than the critical angle, θ_c ($\theta_c = \arcsin [c_+/c_-]$), it is suspected that the incident Čerenkov wavefronts will produce transmitted and reflected wavefronts. For $\theta_- > \theta_c$, critical reflection should occur with no transmitted wave produced.

In cases 5 and 6 the charge produces Čerenkov radiation in both media. One expects the phenomena taking place in these two situations essentially to be combinations of those occurring in cases 3 and 4.

C. Analysis. In all of the following it will be assumed that the reader is familiar with the contents and notation of [1].

In [1] the potential function F was expressed as

$$F = F_p + F^{(1)} + F^{(2)} + F^{(3)}. \tag{2}$$

The expressions for F_p , $F^{(1)}$ and $F^{(2)}$ given in that paper are valid for all cases. The expressions for $F^{(3)}$ (the pole contributions) must be evaluated separately for each case. Thus the remainder of this work will be concerned with evaluating $F^{(3)}$ for each of the four remaining cases.

1. *Case* 3. The disposition of singularities and integration path in the w-plane is shown in Figs. 3, 4 and 5, below, for case 2.

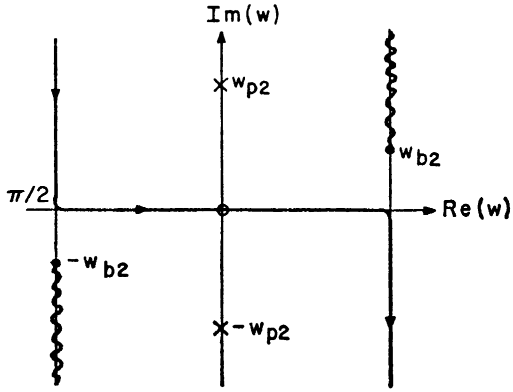

FIG. 3. Poles of $A_-'(w)$, case 3.

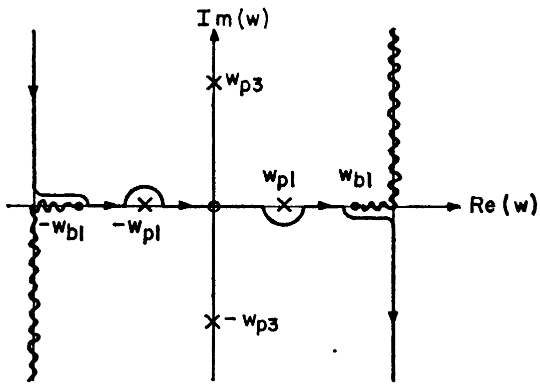

FIG. 4. Poles of $A_+'(w)$, case 3, $w_{p1} < w_{b1}$.

After deforming the integration path [1] we see that the pole at $\pm w_{p1}$ contributes if $|\theta| > w_{p1}$. The values of the pole contributions from $\pm w_{p2}$ and $\pm w_{p3}$ are precisely the same as in case 1.

For $w_{p1} < w_{b1}$, the contribution from $\pm w_{p1}$ is a simple residue term. This term is such that it cancels out F_p in $z > 0$, $|\theta| > w_{p1}$. The resulting wavefront diagram is shown in Fig. 6.

For $w_{p1} > w_{b1}$, Fig. 5 applies. The pole w_{p1} lies on the branch cut. The deformed integration path is shown in Fig. 7. In this case, the contribution from w_{p1} is the sum of one half the residues on the top and bottom of the branch cut. The branch cut integral $f^{(2)}$ is taken in the sense of a principal part at w_{p1}. It again turns out that the contribution from w_{p1} cancels F_p for $z > 0$, $|\theta| > w_{p1}$. The resulting wavefront diagram is shown in Fig. 8.

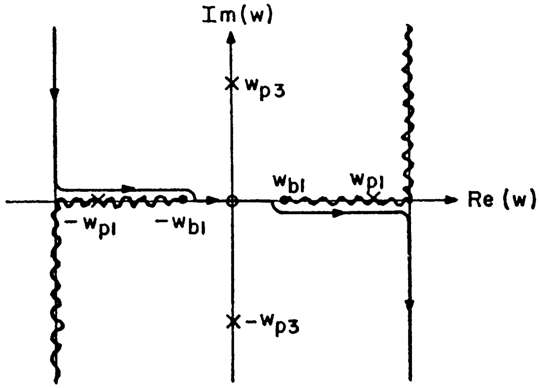

FIG. 5. Poles of $A_+'(w)$, case 3, $w_{p1} > w_{b1}$.

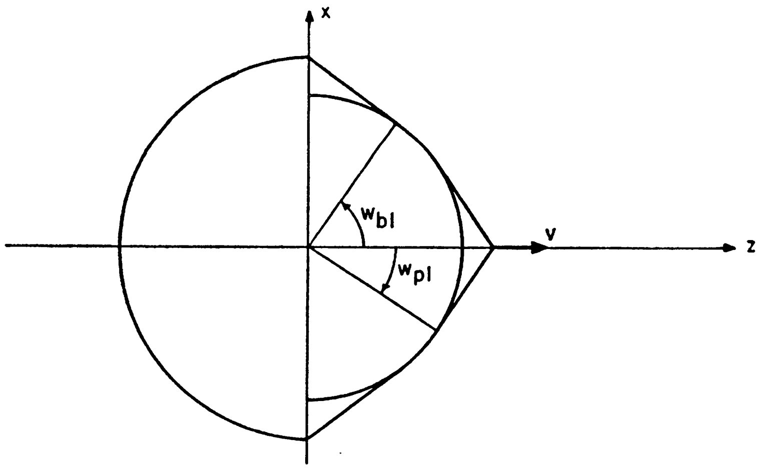

FIG. 6. Wavefront diagram, case 3, $w_{p1} < w_{b1}$.

The analytical expressions for $F^{(3)}$ are given below.
For $z < 0$

$$F^{(3)} = -\frac{(1 + \beta_+^2 - \beta_-^2)^{1/2} - \epsilon}{(1 + \beta_+^2 - \beta_-^2)^{1/2} + \epsilon} \cdot \frac{Q}{2\pi} \arctan\left\{\frac{z + vt}{x(1 - \beta_-^2)^{1/2}}\right\}, \tag{3a}$$

where $\beta_\pm = v/c_\pm$ and $\epsilon = \epsilon_+/\epsilon_-$.

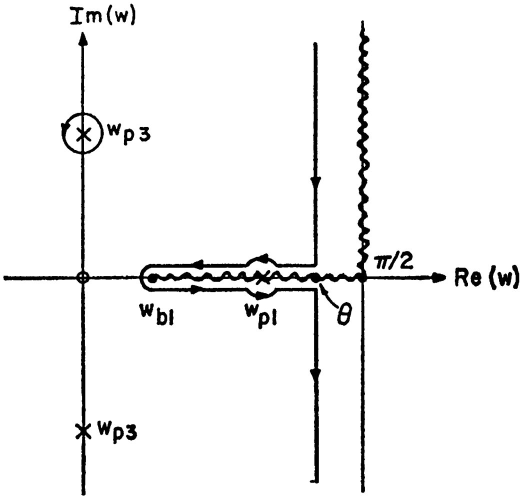

Fig. 7. Integration path for $\theta > w_{p1} > w_{b1}$.

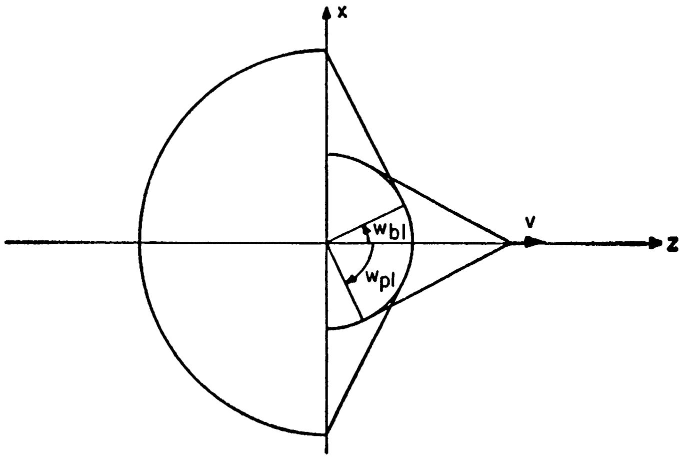

FIG. 8. Wavefront diagram, case 3, $w_{p1} > w_{b1}$.

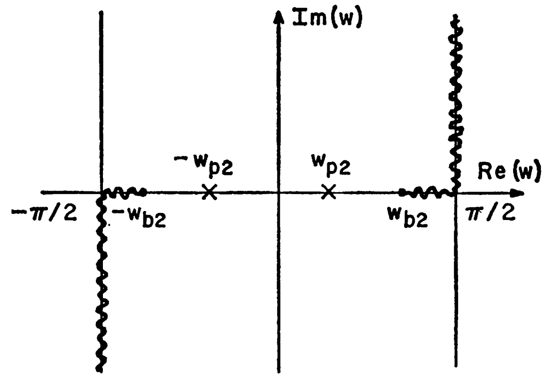

FIG. 9. Poles of $A_{-}(w)$, case 4, $\theta_{-} < \theta_{c}$.

For $z > 0$

$$F^{(3)} = \operatorname{sgn}(x)\frac{Q}{2}u(vt - z - |x|[\beta_+^2 - 1]^{1/2})u(|\theta| - \cos^{-1}[c_+/v]) - \frac{2\epsilon}{(1 + \beta_+^2 - \beta_-^2)^{1/2} + \epsilon}\cdot\frac{Q}{2\pi}\arctan\left\{\frac{z(1 + \beta_+^2 - \beta_-^2)^{1/2} - vt}{x(1 - \beta_-^2)^{1/2}}\right\} \tag{3b}$$

where $u(t)$ denotes the unit step.

Figures 6 and 8 illustrate how the Čerenkov radiation establishes itself in the region $z > 0$ after impact.

2. *Case* 4. The location of poles for $\theta_c > \theta_-$ is shown in Figs. 9 and 10. (Note: $\theta_c = w_{b1}$, $\theta_- = w_{p2}$.) When $\theta_c < \theta_-$ the pole configuration is as shown in Figs. 11 and 12. We see that for $\theta_- > \theta_c$ the pole w_{p3} will never be intercepted. For $\theta_- < \theta_c$, w_{p3} yields

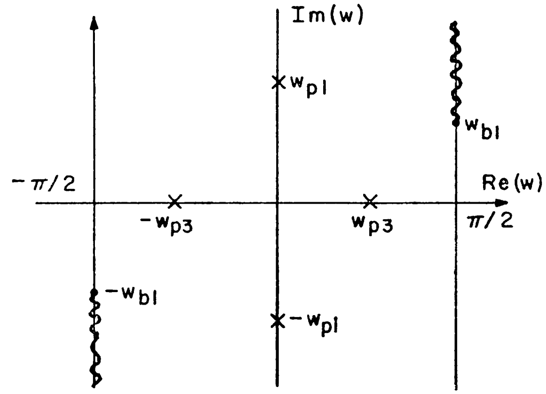

FIG. 10. Poles of $A_+(w)$, case 4, $\theta_- < \theta_c$.

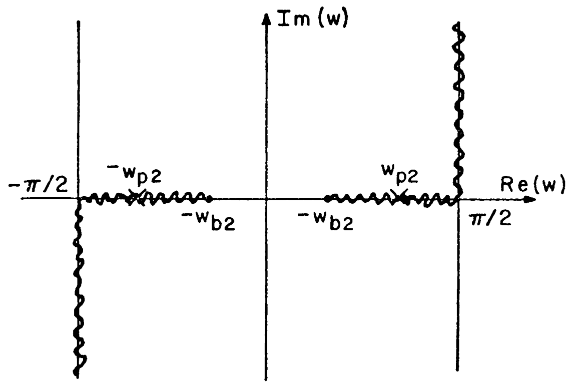

FIG. 11. Poles of $A_-(w)$, case 4, $\theta_- > \theta_c$.

a transmitted wavefront in $z > 0$. The pole w_{p2} yields a reflected wavefront. The wavefront diagrams are shown, below, in Figs. 13 and 14.

For $\theta_- < \theta_c$,

$$F^{(3)} = \frac{\epsilon - (1 + \beta_+^2 - \beta_-^2)^{1/2}}{\epsilon + (1 + \beta_+^2 - \beta_-^2)^{1/2}}\cdot\frac{Q}{2}\operatorname{sgn}(x)u(|\theta| - \theta_-)u(vt - z - |x|[\beta_-^2 - 1]^{1/2}), \quad z < 0 \tag{4a}$$

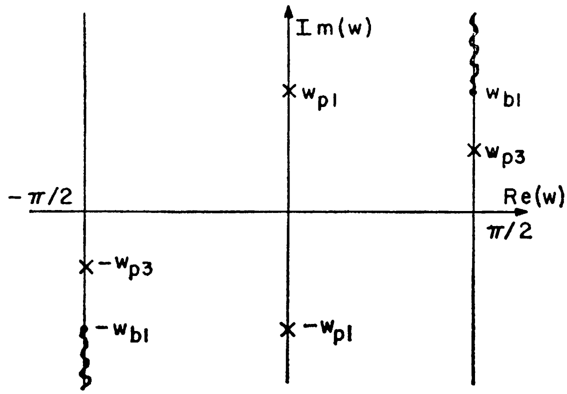

FIG. 12. Poles of $A_+(w)$, case 4, $\theta_- > \theta_c$.

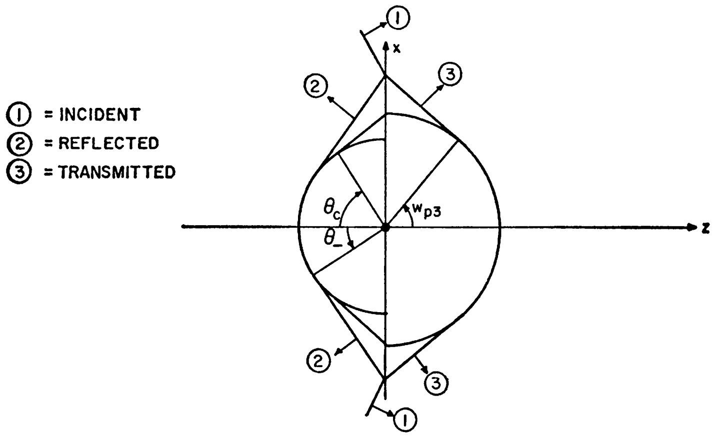

FIG. 13. Wavefronts for case 4, $\theta_- < \theta_c$.

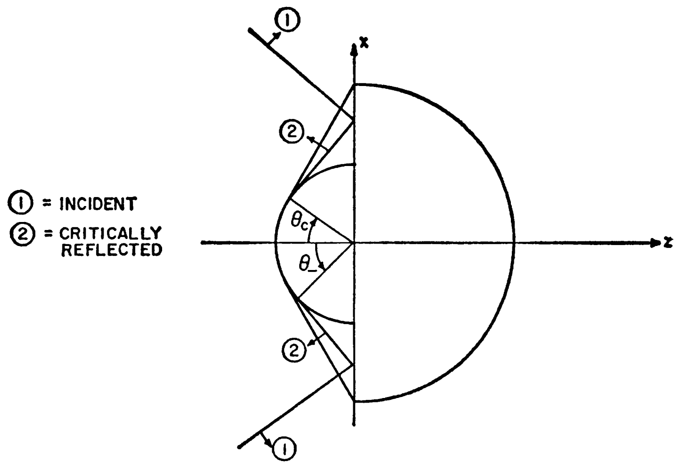

FIG. 14. Wavefronts for case 4, $\theta_- > \theta_c$.

and

$$F^{(3)} = \frac{2\epsilon}{\epsilon + (1 + \beta_+^2 - \beta_-^2)^{1/2}} \cdot \frac{Q}{2} \operatorname{sgn}(x) u\left(|\theta| - \arcsin \left[\frac{c_+}{c_-} - \frac{1}{\beta_+^2} \right]^{1/2} \right)$$

$$\cdot u(vt - z[1 + \beta_+^2 - \beta_-^2]^{1/2} + |x|\,[\beta_-^2 - 1]^{1/2}) + \frac{Q}{2\pi} \arctan \left\{ \frac{z - vt}{x(1 - \beta_+^2)^{1/2}} \right\}, \quad z > 0. \tag{4b}$$

The factors

$$\frac{\epsilon - (1 + \beta_+^2 - \beta_-^2)^{1/2}}{\epsilon + (1 + \beta_+^2 - \beta_-^2)^{1/2}} \quad \text{and} \quad \frac{2\epsilon}{\epsilon + (1 + \beta_+^2 - \beta_-^2)^{1/2}}$$

are just the Fresnel reflection and transmission coefficients for an infinite plane wave incident at an angle θ_- .

For $\theta_- > \theta_c$

$$F^{(3)} = -\frac{1 + \beta_+^2 - \beta_-^2 + \epsilon}{1 + \beta_+^2 - \beta_-^2 - \epsilon} \cdot \frac{Q}{2} \operatorname{sgn}(x) u(|\theta| - \operatorname{arc\,sec} \beta_-) u(vt - z - |x|\,[\beta_-^2 - 1]^{1/2}),$$

$$z < 0, \tag{5a}$$

and

$$F^{(3)} = \frac{Q}{2\pi} \arctan \left\{ \frac{z - vt}{x(1 - \beta_+^2)^{1/2}} \right\}, \qquad z > 0. \tag{5b}$$

3. *Case* 5. For cases 5 and 6 only the results will be given.

For Case 5, $F^{(3)}$ is given by

$$F^{(3)} = \frac{\epsilon - (1 + \beta_+^2 - \beta_-^2)^{1/2}}{\epsilon - (1 + \beta_+^2 - \beta_-^2)^{1/2}} \cdot \frac{Q}{2} \operatorname{sgn}(x) u(|\theta| - \operatorname{arc\,sec} \beta_-) u(vt + z - |x|\,[\beta_-^2 - 1]^{1/2}),$$

$$z < 0 \tag{6a}$$

and

$$F^{(3)} = -\frac{Q}{2} \operatorname{sgn}(x) \Big\{ u(vt - z - x[\beta_+^2 - 1]^{1/2}) u(|\theta| - \operatorname{arc\,sec} \beta_+)$$

$$- \frac{2\epsilon}{\epsilon + (1 + \beta_+^2 - \beta_-^2)^{1/2}} u(vt - z[1 + \beta_+^2 - \beta_-^2]^{1/2} - |x|\,[\beta_-^2 - 1]^{1/2})$$

$$\cdot u\left(|\theta| - \arcsin \left[\frac{c_+^2}{c_-^2} - \frac{1}{\beta_+^2} \right]^{1/2} \right) \Big\}, \qquad z > 0. \tag{6b}$$

The wavefront diagrams are shown in Figs. 15 and 16.

4. *Case* 6. For $z < 0$ and $\theta_- < \theta_c$,

$$F^{(3)} = \frac{\epsilon - (1 + \beta_+^2 - \beta_-^2)^{1/2}}{\epsilon + (1 + \beta_+^2 - \beta_-^2)^{1/2}} \cdot \frac{Q}{2} \operatorname{sgn}(x) u(|\theta| - \theta_-) u(vt + z - |x|\,[\beta_-^2 - 1]^{1/2}) \tag{7a}$$

For $z > 0$ and $\theta_- < \theta_c$,

$$F^{(3)} = -\frac{Q}{2}\,\mathrm{sgn}\,(x)\Big\{u(vt - z - x[\beta_+^2 - 1]^{1/2})u(|\theta| - \operatorname{arc\,sec}\beta_+)$$
$$-\frac{2\epsilon}{\epsilon + (1 + \beta_+^2 - \beta_-^2)^{1/2}}\,u(vt - z[1 + \beta_+^2 - \beta_-^2]^{1/2} - |x|\,[\beta_-^2 - 1]^{1/2})$$
$$\cdot u\left(|\theta| - \arcsin\left[\frac{c_+^2}{c_-^2} - \frac{1}{\beta_-^2}\right]^{1/2}\right)\Big\}. \tag{7b}$$

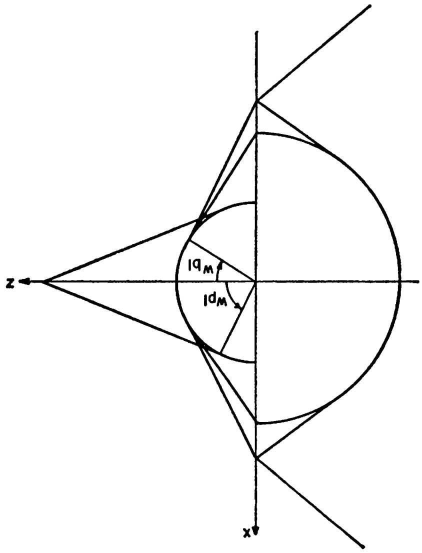

FIG. 15. Case 5, $w_{p1} > w_{b1}$.

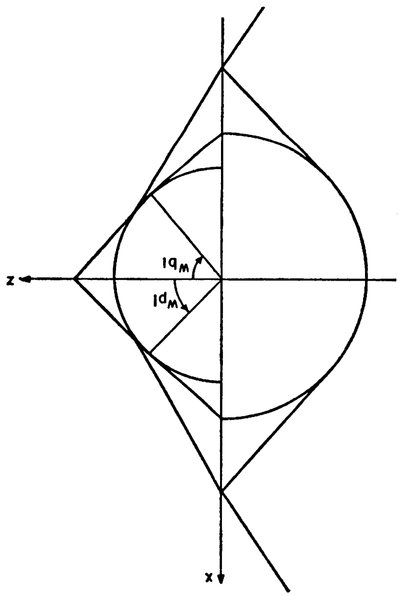

FIG. 16. Case 5, $w_{p1} < w_{b1}$.

For $z < 0$ and $\theta_- > \theta_c$,

$$F^{(3)} = -\frac{1 + \beta_+^2 - \beta_-^2 + \epsilon}{1 + \beta_+^2 - \beta_-^2 - \epsilon} \cdot \frac{Q}{2} \operatorname{sgn}(x)(|\theta| - \theta_-) u(vt + z - |x| [\beta_-^2 - 1]^{1/2}). \tag{8a}$$

For $z > 0$ and $\theta_- > \theta_c$,

$$F^{(3)} = -\frac{Q}{2} \operatorname{sgn}(x) u(vt - z - |x| - [\beta_+^2 - 1]^{1/2}) u(|\theta| - \operatorname{arc\,sec} \beta_+). \tag{8b}$$

The wavefront diagrams for case 6 appear in Figs. 17 and 18.

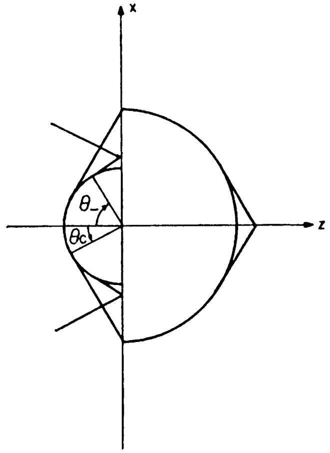

FIG. 17. Case 6, $\theta_- > \theta_c$.

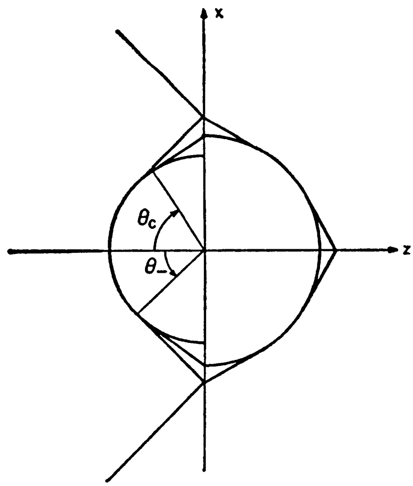

FIG. 18. Case 6, $\theta_- < \theta_c$.

REEFRENCE

1. E. Ott and J. Shmoys, *Transient aspects of transition radiation*, Quart. Appl. Math., (4) **25**, 377–398 (1968)